

Modeling medium and low voltage grids using population density

Emile Emery , Joseph Le Bihan , and José Halloy 
Université Paris Cité, CNRS, LIED UMR 8236, Paris, F-75006, France
(Dated: February 17, 2026)

The expansion of global electricity distribution systems necessitates the deployment of massive infrastructure. Assessing its implications from a spatial and material perspective requires an understanding of the core drivers of a distribution grid configuration. Our model samples substation locations using a non-linear relationship with population density and constructs the network applying the Kruskal algorithm. This streamlined approach generates realistic grid structures at the local scale and provides accurate estimates of the total network length at the national scale. Using highly granular population data, this local model reveals a profound connection between population spread and distribution grid, which appears to persist at the global level. Potentially driven by the emergent properties of population scaling laws, the full network characteristics appear to be well described by multivariate power laws on aggregated population and area. Validated across 35 countries, these results provide new multi-scale tools for characterizing electrical infrastructure and reveal key determinants of distribution grid extent.

I. INTRODUCTION

Electricity transmission and distribution networks contain a substantial share of the in-use stocks of copper and aluminum within society [1]. This share is expected to increase by an order of magnitude over the coming decades as electrification grows and electricity consumption rises [2]. Characterizing the length and configuration of these networks therefore becomes a critical issue, as it enables, on the one hand, a refined estimation of the quantities of materials required for future network expansion and, on the other hand, an assessment of the location and magnitude of existing stocks from a potential recycling perspective.

Electrical power systems are structured in hierarchical layers, each serving distinct contributions to the transport of electricity from production sites to end consumers [3]. The transmission network operates at the highest voltages to transport power over long distances with minimal losses. It comprises two sublayers: Extra High Voltage (EHV) networks (around 200-1000 kV) that interconnect major production centers with major consumption areas such as administrative regions, and High Voltage (HV) networks (around 45-200 kV) that transfer power from EHV to cities, industrial clusters, and large rural areas. The distribution network completes the delivery chain, operating at lower voltages to supply electricity to residential and small industrial consumers. It is divided into two distinct layers: the Medium Voltage (MV) network, operating at tens of kV, connects HV substations from the transmission layer to numerous local MV/LV substations and some industrial consumption nodes; and the Low Voltage (LV) network, operating around 400V, delivers power from these local substations directly to end users: households, factories, and commercial buildings.

The transmission segment of electricity networks is already relatively well documented, first because it

involves much shorter total cable lengths, and second because it is largely determined by the spatial distribution of electricity generation sites [4]. Moreover, this segment is generally managed by a limited number of large operators (Transmission System Operators, TSOs), which facilitates data aggregation and transparency. In contrast, the distribution segment covers significantly greater lengths and is often operated by a large number of local entities (Distribution System Operators, DSOs), making the collection and harmonization of local data considerably more complex. In addition, information on the location of power cables and substations can be sensitive, which further limits access to these data. France constitutes a notable exception, as a single DSO manages the vast majority of the distribution network. This distinction between transmission and distribution networks is also reflected in material composition: for physical and technical reasons, transmission networks are predominantly composed of aluminum conductors, whereas distribution networks primarily rely on copper cables [5].

Several methods have been employed to describe and model electricity distribution networks. This task is far from straightforward; Zvoleff *et al.* notably demonstrated that an identical number of nodes, or substations, to be supplied can result in fundamentally different network configurations depending on the spatial distribution of their locations. The network could be composed mainly of short segments (nucleated population) or could require long cables between dispersed areas [6]. Various studies based on satellite imagery—such as night-time light intensity [7] and rooftop detection [6]—have produced satisfactory results, but they suffer from notable limitations. In particular, these approaches tend to inadequately capture network connections in rural areas.

The literature suggests that electricity networks tend to follow a set of general organizing principles, in

particular the optimization of an overall system cost. This cost encompasses, among others, installation costs, Joule losses, and reliability considerations and explains the observed topologies [4, 8, 9]. While satellite imagery provides a direct way to identify the number and spatial distribution of grid-connected structures, it requires substantial processing effort. Population density appears to be a much simpler proxy for the spatial distribution of structures to be connected, and potentially a powerful one [7, 10]. This approach is particularly relevant for countries with a “mature” electricity network, where nearly 100% of the population has access to household electricity. Although the theoretical derivation of the relationship between population density, the number of substations, and the various optimization logics governing network design remains challenging, the availability of detailed data for France makes it possible to propose a network model driven by population density as an input, combined with a parsimonious set of assumptions calibrated to reproduce the French distribution network.

This relationship between population density and distribution network configuration seems to remain valid for other countries with full electrification, and enable relatively precise estimates of the spatial distribution of in-use copper stocks at the national scale and of future grid material demand. Population density data and projections are effectively far more accessible and well-developed than data on electricity distribution networks, which in some cases are simply unavailable.

Objectives

We aim to develop a model capable of estimating the spatial layout of an MV network and the order of magnitude of the total cable length required for a complete electrical distribution network. The main assumption is that electrical demand correlates well with population density in space.

The objectives of this study are as follows:

- To develop a model capable of generating a spatially explicit representation of the French medium-voltage electricity distribution network, using population density over the entire territory as the sole input.
- To assess the accuracy of this model in the French case across several dimensions, including network topology, the spatial location of network nodes and edges, as well as aggregated metrics such as total medium-voltage line length or total number of nodes (substations).
- To evaluate and discuss the relevance of applying this model, calibrated on the French case, to other countries.

- Based on the results obtained for other countries using this model calibrated on France, to discuss the invariants and the driving factors of aggregated quantities such as total medium-voltage and low-voltage line lengths, or the number of substations, in particular in relation to aggregated indicators such as population, land area, and electricity consumption.

II. MODEL

Electricity distribution networks typically exhibit tree-like structures[9]. Using this observation as a modeling assumption, a set of spatially explicit nodes (substations) can be transformed into a network. The key question then becomes how to model the number and spatial distribution of these nodes based on population density. We hypothesize the existence of a direct relationship between node density n_{node} and population density ρ across space : $n_{node} = \frac{N_{node}}{S_{cell}} = f(\frac{N_{pop}}{S_{cell}}) = f(\rho)$. In the French case, comparing node density with population density at a fine spatial resolution makes it possible to identify and calibrate this relationship.

The WorldPop database provides an estimated population density per grid cell (people per km^2) for all countries, with a resolution of 30 arc seconds [11]. This data was produced using random forest-based machine learning techniques to disaggregate governmental population counts from administrative units into grid cells [12–14]. The lattice has a fine resolution and captures the nucleation of households, which are crucial for network length measurements [6]. These data will serve to calibrate the model on the French case and as input to provide a spatial representation of developed electrical distribution networks, thereby estimating their total length for the other countries.

Regarding the set of nodes, the French DSO ENEDIS covers over 95% of the French territory [15] and provides an open database containing the locations of all its MV/LV substations in the French territory [16]. Unfortunately, these nodes correspond only to substations connecting the MV network to the LV network, and do not include the terminal nodes or end-use structures, such as households, where the LV network terminates. ENEDIS provides, in addition to data on network nodes, a set of line-shaped drawings (capturing cables’ location); however, these two datasets are not harmonized. Thus, the spatial accuracy of the line trajectories is insufficient to directly reconstruct the full network topology, *i.e.*, the connectivity of substations [17]. This lack of internal consistency further underscores the need for modeling approaches such as the one developed in the present study. In this study we restrict our analysis, in a first step, to modeling the MV network, for which a complete set of nodes is available. Nevertheless, using

population density to estimate the number and spatial distribution of terminal nodes appears to be a promising, potentially more effective approach.

The main difficulty in estimating node density as a function of population density is that WorldPop data are provided in a gridded spatial representation (square cells), which introduces potential edge effects. This, in turn, induces a stochastic component in the relationship. In addition, the actual locations of substations themselves are likely to exhibit an intrinsic degree of randomness, as factors other than population density may locally influence their placement while having a negligible effect on average (for instance, the presence of a lake within an urban area preventing the installation of substations in part of a grid cell).

Accordingly, Figure 1 depicts the average density of substations as a function of average population density, defined as the mean number of substations computed across all WorldPop cells corresponding to a given population density. This relationship therefore describes the expected value of the number of substations. Two distinct regimes are observed, with a break in slope around a critical density of approximately 8 inhabitants per km^2 . The fitted relation is the following :

$$n_{\text{stat}}(\rho) = \begin{cases} 0.07\rho & \text{if } \rho < 8 \text{ hab}/\text{km}^2 \\ 0.2\rho^{0.5} & \text{if } \rho \geq 8 \text{ hab}/\text{km}^2. \end{cases} \quad (1)$$

This result is consistent with intuition: in sparsely populated areas, the number of substations is approximately proportional to the number of inhabitants, whereas in densely populated areas, scale effects emerge, making the number of substations markedly sublinear. This effect is closely related to the use of fixed-area density measures; reversing the perspective—by allocating a serviced area to each substation—eliminates this break (cf. appendix A).

To account for the stochastic effects described above, and in particular to adequately represent the large number of cells containing no substations, we adopt a Poisson distribution. This choice is motivated by its simplicity, the absence of additional parameters, and its widespread use in counting processes. Figure 3, which shows the proportion of cells without substations as a function of population density, supports the suitability of this probabilistic assumption.

At this stage, the algorithm samples substations' locations cell by cell. For each cell i , a random draw N_i is performed according to a Poisson distribution with parameter $n_{\text{stat},i} = f(\rho_i)$, where ρ_i denotes the population density of the cell i as provided by WorldPop, and f is defined in Figure 1. This draw determines the number of substations N_i to be placed in cell i ; these

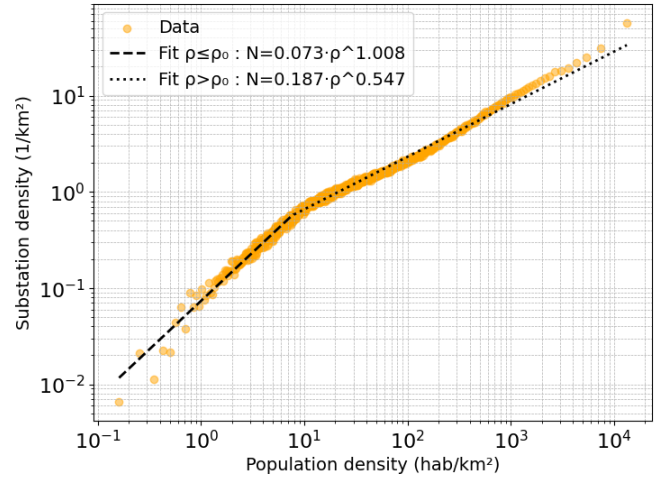


Figure 1: Empirical relationship between the number of substations in a cell and the corresponding population density. Each point corresponds to the average number of substations per bin of density. The bin set is chosen such that each bin contains around 1000 data points.

The threshold value is $\rho_0 \simeq 7.948$.

substations are then randomly and uniformly positioned within the cell. This Poisson distribution naturally models the discrete, random nature of node placement and the observed cell-to-cell fluctuations around the mean density, allowing for the recovery of a realistic node sprinkling from a grid-cell dataset (cf. appendix A).

We assume that building a new substation (HV/MV or MV/LV) and laying kilometers of lines are both costly, and the network seeks an optimal configuration that minimizes costs while maintaining a sufficient service quality [8]. By 'costly', we mean all costs, not just the direct building cost (e.g., the electricity loss associated with a particular configuration). Having a node position dataset, we can connect the substation using a minimum spanning tree algorithm. In real distribution networks, it is cost-effective to add loops to the tree structure: when the nodes are connected to the rest of the network through at least two paths, it is safer and more effective in terms of Joule losses [18]. Nevertheless, the contribution of bridges' length to the network's total length is weak, and the tree-like structure serves as a suitable first proxy for estimating the overall spatial layout and material content of an MV grid [19]. The second-order corrections to the total cable length estimates are given in appendix B.

III. RESULTS

This Results section is naturally structured into three subsections, progressing from a local to a global perspective.

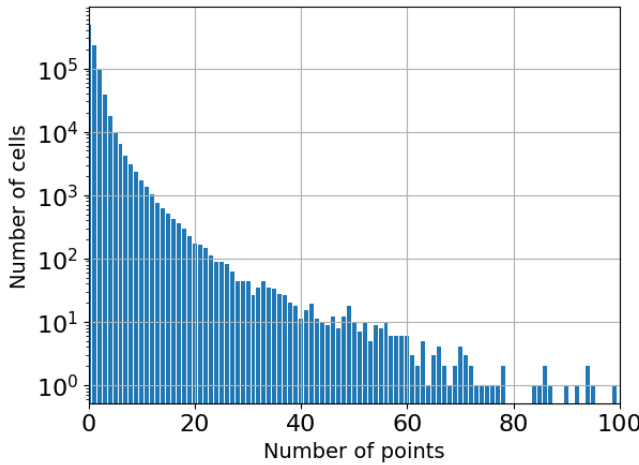


Figure 2: Histogram of the number of nodes in grid-cells.

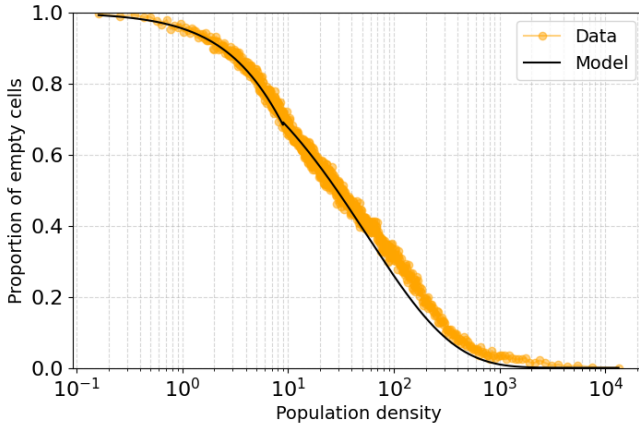


Figure 3: Proportion of empty cells in the data for all population density values.

tive on the relationships between population, spatial organization, and the electricity grid. First, focusing on the French case, we compare the outputs of the proposed model—based on population density data at a 30 arc seconds (approximately 0.59 km^2 at French latitude) spatial resolution—with the existing electricity network. The similarity between the generated and observed networks is assessed qualitatively through local-scale visual inspection and quantitatively using aggregated indicators at the global scale. The close agreement between the model-generated network and empirical data confirms the strong relationship between network structure and the spatial distribution of population. Moreover, the model’s construction enables this relationship to be consistently captured at both local and global scales.

Second, we apply this network generation process, calibrated on the French case, to other countries for which detailed local grid data are unavailable but aggregated network statistics are available. The analysis of these results enables an assessment of the degree of generality of

the relationship between electricity networks and population distribution, as well as an evaluation of the extent to which a model calibrated at the local scale in France can reproduce macroscopic quantities (eg., total network length) in other national contexts.

Finally, we investigate this relationship directly at the global scale by examining, among other variables, aggregated measures of territorial area and population (number of households) in relation to the total lengths of different voltage classes across a large number of countries. This approach leads to the emergence of simple yet highly effective scaling laws that capture a degree of universality at the macroscopic level.

A. Generating the French MV network from sole population density

1. Visual comparison at the local scale

Figure 4 shows the locations of the network nodes generated by the model together with the actual locations of nodes across the entire territory. A strong similarity is observed at both local and global scales.

The white areas in the map shown in the upper part of Figure 4 (empirical data) correspond to territories where the electricity grid is not operated by the dominant network operator (ENEDIS), and for which spatial data are therefore unavailable. This artifact does not naturally appear in the model output (lower part of Figure 4), as the model does not account for differences in network operators.

Figure 5 no longer displays individual nodes but instead shows the full set of edges generated by the model, together with a comparison to the actual line drawings provided by the grid operator ENEDIS. In this case, the spatial traces are not exactly coincident; however, they exhibit a similar network topology. In particular, the empirical network follows a structure very close to a tree topology. Since the model is explicitly constrained to generate a tree, it consequently produces a network that is topologically consistent with the observed one.

By contrast, the edges are not necessarily spatially positioned with the highest precision. In particular, we observe a specific effect induced by the road network: a fraction of substations and the majority of power lines are aligned along roads. Population density can partially account for this effect, as roads tend to pass through cities and villages with higher population density, but it fails to do so outside inhabited areas.

Another, more subtle, topological feature of the real network is the presence of *bridges*, that is, connections between nodes that are already indirectly connected through two branches of the tree. This addition of links relative to a purely tree-like topology provides a degree of resilience to the real network. These bridges are visible through the loops present in the right-hand panel of Figure 5 but absent in the left-hand one. Account-

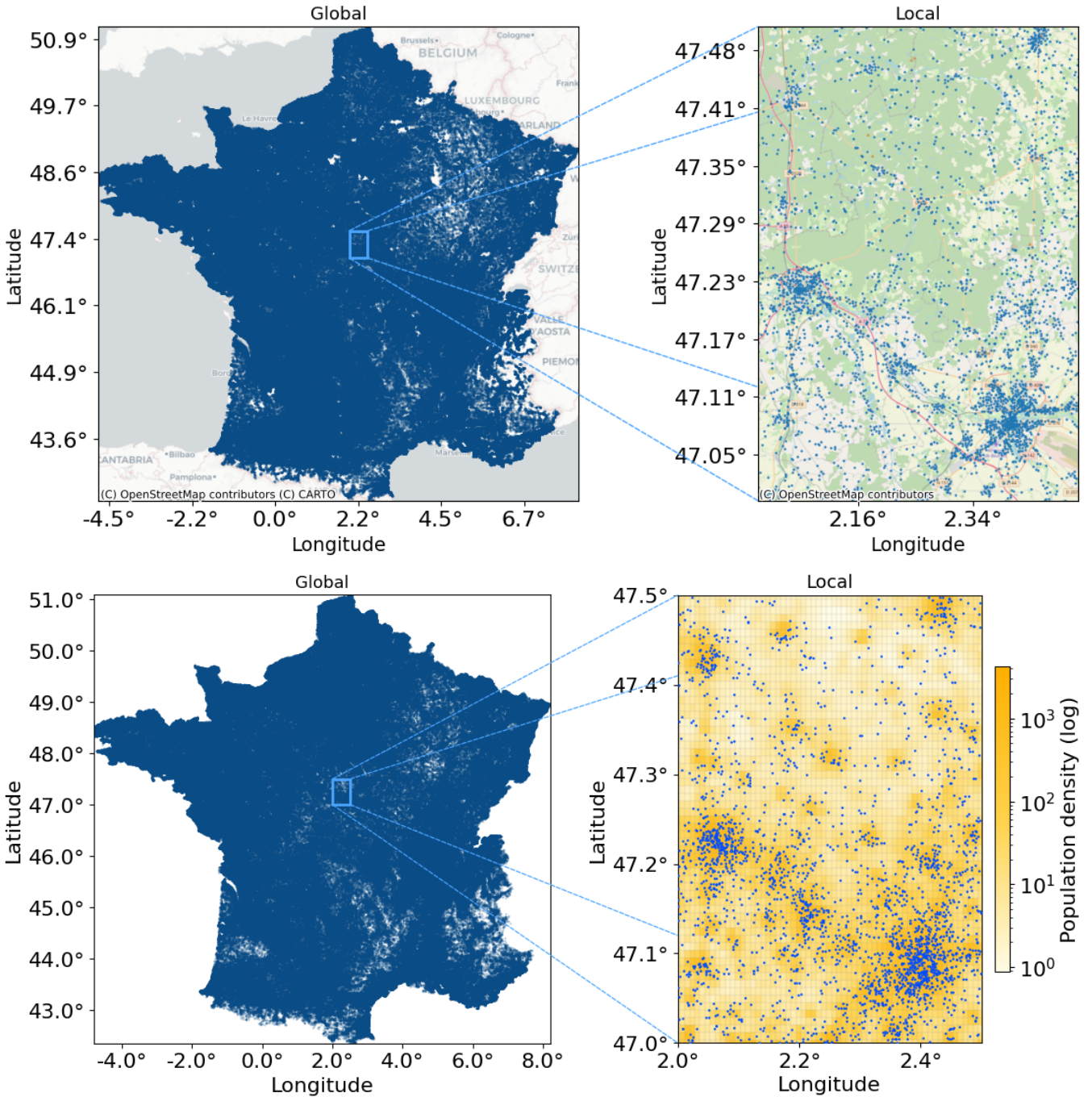


Figure 4: Node spatial distribution for the empirical dataset (top figure), and the model (bottom figure). The white holes in the top figures corresponds to area that are not managed by ENEDIS.

ing for this specific feature would require adapting the node-connection algorithm.

In these respects, it is important to emphasize that the generated output represents a “typical” network corresponding to the population distribution. This network accurately captures the locations of substations and connectivity patterns, but it does not aim to predict whether an actual cable passes through given spatial coordinates. Nevertheless, the generated network is expected to pro-

vide reliable values for aggregated indicators computed over spatial extents of at least 0.59 km^2 (the resolution of the population grid). If the generated network reproduces the correct topology and node spatialization, then highly local effects (eg., those induced by specific basement layouts) should average out at larger spatial scales.

Finally, unlike ENEDIS, which as previously mentioned provides two distinct datasets (nodes and lines drawings), this model produces a fully consistent network

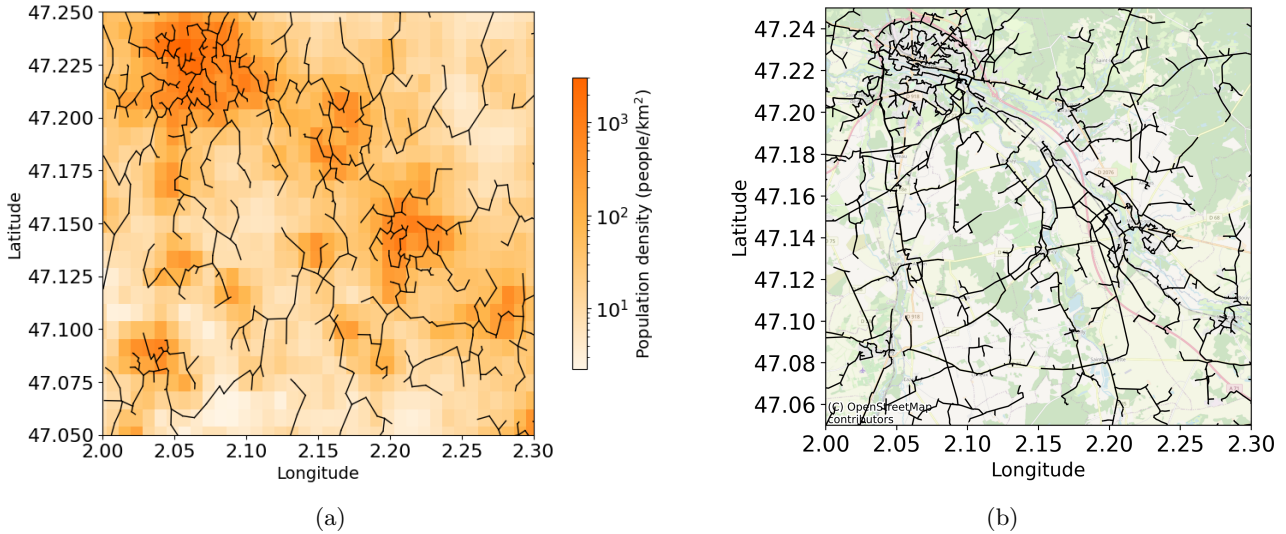


Figure 5: (a) Real population density data in France (orange) with simulated nodes (blue), minimum spanning tree edges (black), and computed Voronoi diagram (grey). (b) Real-world distribution grid layout in the corresponding area, with blue nodes representing MV/LV substations and black edges indicating MV lines.

composed of both nodes and edges, with a well-defined topology.

2. Quantitative features at the country scale

The underlying hypothesis of this work—that the electricity network is determined, or at least strongly correlated, with the spatial distribution of population—appears to be confirmed at the local scale in the French case, where the network clearly follows the population density field. A natural question is whether the effectiveness of the proposed modeling approach at the local scale is preserved at the global scale when considering aggregated network characteristics. In particular, we focus on two essential quantities: the total length of the network and the number of substations.

This is by no means guaranteed *a priori*. Regarding the number of substations, the model is parameterized using this quantity, and one may therefore expect to recover a total number of substations close to the empirical value. However, the total number of substations is not imposed as a direct constraint. First, the parameterization concerns the expected number of substations as a function of the population density within a cell, which is itself modeled using a weakly parameterized power-law relationship. Concerning the second feature, the total network length is not incorporated into the model parameterization at all; it emerges solely from the tree structure applied to stochastically sampled nodes.

Table I presents a comparison between the values of these quantities computed from the generated model and the experimental data obtained for the actual network. While the accuracy of the estimated total number of nodes (88%) is not particularly surprising, the accu-

	$N_{stat} (10^5)$	$L_{MV}^{route} (10^5 \text{ km})$	$L_{MV}^{cable} (10^5 \text{ km})$
Literature	7,87	n.d.	6,45
Model	8,79	3,94	6,06
Error	12%	n.d.	6%

Table I: French aggregated indicator comparison

The total number of substations and the total cable length computed from the generated network are close to the values reported in the literature (*cf* appendix B for details on the error corrections).

racy of the total network length (94%) highlights a key strength of the model: at the global scale, the local discrepancies in line routing observed in Figure 5 have no impact or effectively compensate for one another. That is, the difference in total line length within a given area (e.g., between Figures 5a and 5b) is consistently very small, or the over- and under-estimation errors offset each other when aggregated over the entire French territory. In both cases, the generated network can therefore be interpreted as a representative or “typical” network that preserves both the local visual structure and the values of global network characteristics.

The model constructed for the French case thus establishes a strong link between population distribution and the electricity network at both local and global scales. This suggests that a simple local population–network relationship is sufficient to iteratively (“cell by cell”) construct a global network that closely approximates the real one. Beyond the network generation process itself, which may be valuable for future research or prospective studies on network deployment, this result indicates that, despite (i) the geographical, social, and historical diversity of the various territories composing France and (ii) the

presence of actors and potential constraints operating at the national rather than the local level, a single local relationship is, on its own, sufficient to characterize the structure of the electrical network across all local areas as well as at the national scale.

B. Results for other countries

This correlation law between population density and the density of electrical substations, therefore, appears to provide an effective description of the current French power grid. A natural subsequent question is whether this descriptive capability remains valid at other points in time or in other countries. Regarding spatial extension, the following section presents a first comparison of the model results across approximately 30 countries. In principle, the model output would allow comparisons at the local scale and analysis of differences in network topology and substation locations between France and other countries. Unfortunately, the lack of access to local-scale data on electrical networks in other countries has prevented such a comparison.

Nevertheless, as in the French case, this approach still makes it possible to compute the global characteristics of the power grid (total number of substations and total network length) from the model results, and to compare them with values reported in "white" or "grey" literature for the different countries, which are available for all selected cases. These quantities must, however, be interpreted with caution, as they are sometimes derived from estimates based on strong underlying assumptions. In order to ensure that this comparison is as meaningful as possible, we selected countries for which the relevant data were available and that exhibit an electricity access rate similar to that of France (access to electricity for 100% of the population as defined by the World Bank [20]). This factor, therefore, cannot account for potential differences relative to the French case, which must instead be sought in the manner in which the networks are organized.

Figures 6 and 7 present a comparison between the total number of substations and the total network length computed from the model outputs—generated using each country's local population density and a model calibrated on the French case (y -axis)—and the corresponding values reported in the "white" or "grey" literature (x -axis). These figures should be interpreted as follows: each point represents a country; the closer a point lies to the line $y = x$, the closer the model-derived value is to the value reported in the literature. Points above this line indicate model overestimation, whereas points below it indicate underestimation.

The substantial disparity in magnitudes across countries makes a log-log representation visually more meaningful, but it also considerably weakens the interpretability of the R^2 metric, which is almost entirely driven by the extreme values in the distribution tail (e.g., India, the

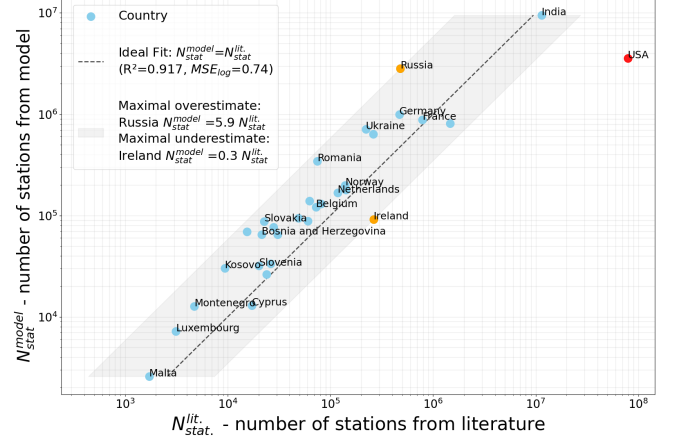


Figure 6: Comparison of total $N_{stations}$ value computed on model output and estimation from literature.

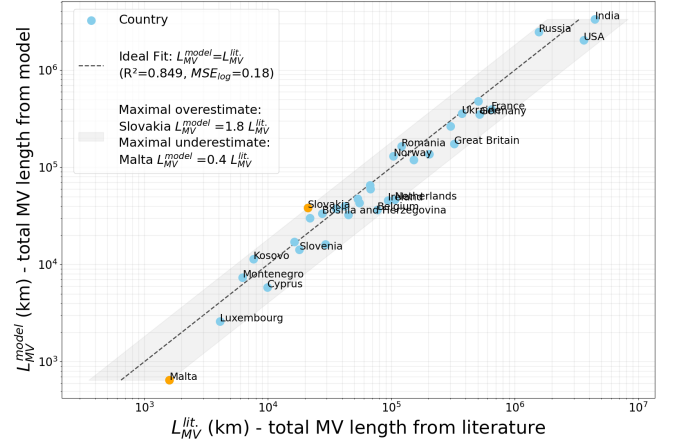


Figure 7: Comparison of total L_{MV} value computed on model output and estimation from literature. It represents the total MV network lengths reported in the literature and those computed by the model. As it is often unclear whether the values reported in the literature refer to route length or cable length, and how the latter is calculated, we chose in this case to use as model output the direct sum of segment lengths, without applying any correction factors (cf appendix B).

United States, or Russia) that dominate the remaining data points. In this context, it is therefore more appropriate to consider the mean squared logarithmic error (MSE_{log}), which penalizes relative deviations and is independent of the order of magnitude of the values. This indicator is computed as follows :

$$MSE_{log} = \frac{1}{N_{countries}} \sum_{i \in \text{Countries}} \log \left(\frac{y_{\text{model},i}}{y_{\text{lit.},i}} \right)^2. \quad (2)$$

With respect to the number of substations, Figure 6 shows that, despite a relatively high R^2 , the model ex-

hibits a substantial logarithmic error. Both a significant bias—manifested as a tendency of the model to overestimate the number of substations (points lying on average above the line $y = x$)—and considerable dispersion are observed. The United States of America, which was excluded from the dataset used for the calculations, shows a discrepancy of two orders of magnitude relative to the model output, highlighting the non-universal nature of the relationship employed.

In fact, there appear to be “two basic models for distribution systems, the European and the American, with combinations of the two employed by various countries. These models use different mixtures of distribution transformers, with the European system having a higher concentration of larger-capacity, higher-voltage MV transformers and fewer small units, while the American system has a large number of small units located closer to the customer.” [21]. This design difference, which translates into a substantial discrepancy in the number of substations at the macro level, necessarily also affects the network’s local configuration. The precise correlation between substation and population density identified for France does not appear to hold in some of the other countries, where variations in substation types may influence both their numbers and the overall network architecture. It can nevertheless be hypothesized that countries for which the model closely matches the literature values actually exhibit a distribution system design similar to that of the French case.

With respect to the total medium-voltage network length, Figure 7 shows a much closer agreement between the model results and the literature values, despite a lower R^2 . Only a small bias is observed, with a slight tendency toward underestimation, and the points are highly concentrated around the line $y = x$. This finding is notable given the disparities in N_{stat} and, consequently, in the local network configuration. It appears that, despite differences in the topologies of foreign networks, the model calibrated on the French case provides a fairly accurate estimate of the total length of the medium-voltage network. This may suggest that the nature and number of transformers have relatively little impact on the total network length, which instead appears to correlate strongly with the population’s spatial distribution.

C. Macro-level indicators estimation

The relationship between population—sometimes measured by the number of households—and the total length of electrical network cables is not new and has been highlighted in the literature [6, 7, 22–24]. However, there is no consensus on how to characterize this relationship. Kalt *et al.* employ a linear regression with respect to the number of households connected to electricity and the country’s electricity consumption to estimate the total length of the distribution network [22]. Other authors, such as Kuhnert and Bettencourt, observe an empirical power-

law relationship between the length of low-voltage cables and population in densely urbanized areas of Germany, with an exponent ranging from 0.81 to 0.92 [23, 24].

It is noteworthy that in these previous formulations, the spatial dimension (geographic dispersion of the population) does not appear to affect the total cable length. This naturally raises questions, as it seems intuitive that the same population spread over a larger territory would require a more extensive network, and thus a greater total cable length. In the case of Kuhnert and Bettencourt, the absence of a spatial effect may be explained by the restriction of their study to dense urban areas, thereby limiting its spatial extent. Nevertheless, it seems reasonable to observe a sublinear scaling law in cities, since urban networks, regardless of their nature, exhibit fractal characteristics [25], capturing scale effects that a linear relationship cannot. Indeed, a clearly sublinear exponent is also observed in the model calibration for urban areas (see Section II).

This local-scale power-law relationship, as shown in the previous section, enables relatively accurate estimates of the length of the medium-voltage network. Given the existence of general empirical laws governing how populations occupy space, whether in urban or rural areas [4, 26], it appears feasible to extend this relationship from the local to the global scale, linking population and national land area through these spatial distribution patterns. While an explicit bottom-up construction may seem complex and inconsistent with the derivation of the local relationship—which relies on an empirical average in the French case—the following section presents multi-variable power-law regressions incorporating population (measured by the total number of households) and national surface area, along with a discussion of the impact of other variables such as electricity consumption.

1. Powerlaw-scaling of the number of substation - N_{stat}

Consistent with the observations of the previous section, N_{stat} , which was poorly captured by the model due to the existence of multiple possible network architectures, is also relatively poorly described by a multi-variable power-law regression involving population, national surface area, and electricity consumption. The regression yielding the best performance is:

$$N_{stat} = 0.07 \text{ } Pop^{0.75} \text{ } Area^{0.22}. \quad (3)$$

However, it is characterized by unsatisfactory values of both $R^2 = 0.63$ and $MSE_{log} = 0.32$. This confirms that, without specifying the underlying network architecture, it is difficult to relate population density to substation density at the global scale.

2. Powerlaw-scaling of the medium-voltage length - L_{MV}

By contrast, and in line with the model’s results, the medium-voltage network length is particularly well described by power-law relationships involving global variables. The equation providing the best fit is the following :

$$L_{MV} = 0.05 \text{ Pop}^{0.6} \text{ Area}^{0.35} \text{ Conso}^{0.13}, \quad (4)$$

with $R^2 = 0.91$ and $MSE_{\log} = 0.076$. However, an even simpler formulation that does not include electricity consumption yields estimates of nearly identical accuracy:

$$L_{MV} = 0.17 \text{ Pop}^{0.59} \text{ Area}^{0.36}, \quad (5)$$

with $R^2 = 0.94$ and $MSE_{\log} = 0.081$. Figure 8 compares the results of this power-law relationship (y -axis) with the values reported in the literature (x -axis) for the countries considered. A correlation is observed that is even stronger than that obtained from the model-based results. The relatively minor impact of explicitly accounting for electricity consumption is a noteworthy finding, which is discussed further in the next section.

3. Powerlaw-scaling of the low-voltage length - L_{LV}

Although our model focuses on the medium-voltage network—primarily due to the availability of local-scale data only for this voltage class—the works of Kalt *et al.* and Bettencourt suggest that the relationship between population and cable length may also hold at the low-voltage level [22, 23]. Following this line of reasoning, we applied the same power-law fitting procedure. The equation providing the best fit is :

$$L_{LV} = 0.4 \text{ Pop}^{0.66} \text{ Area}^{0.22} \text{ Conso}^{0.26}, \quad (6)$$

with $R^2 = 0.76$ and $MSE_{\log} = 0.14$. These results suggest that, in contrast to L_{MV} , the low-voltage network length depends less strongly on the total surface area of the country. This observation is consistent with intuition: the low-voltage network represents the “last layer” of the distribution tree, located close to where people actually reside, regardless of how geographically dispersed population clusters may be.

4. Correlation between L_{LV} and L_{MV}

A fairly strong correlation is also observed between the lengths of low-voltage and medium-voltage cables. Kalt *et al.* assume that low-voltage cables account for 63% of the total length of distribution network cables. By fitting the low-voltage length as a function of the medium-voltage length, we obtain a coefficient of 1.63 ($R^2 = 0.96$, $MSE_{\log} = 0.14$), indicating that the low-voltage length is 1.63 times greater than the medium-voltage length. This corresponds to a share of $\frac{1.63}{1+1.63} = 62\%$, which is close to the value reported by Kalt *et al.*

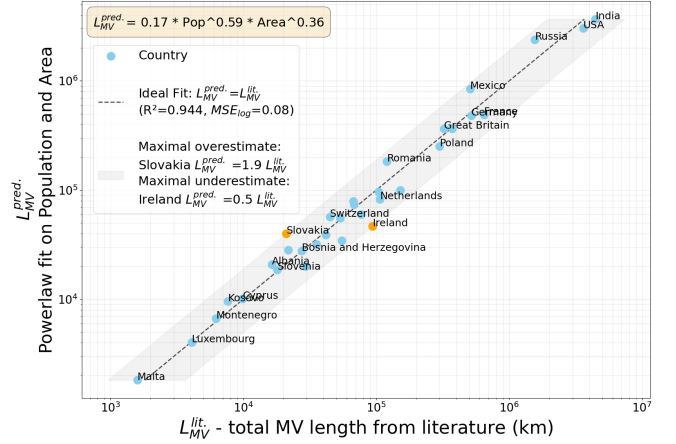


Figure 8: Estimation of total L_{MV} value using powerlaw relationship on country’s total population and area.

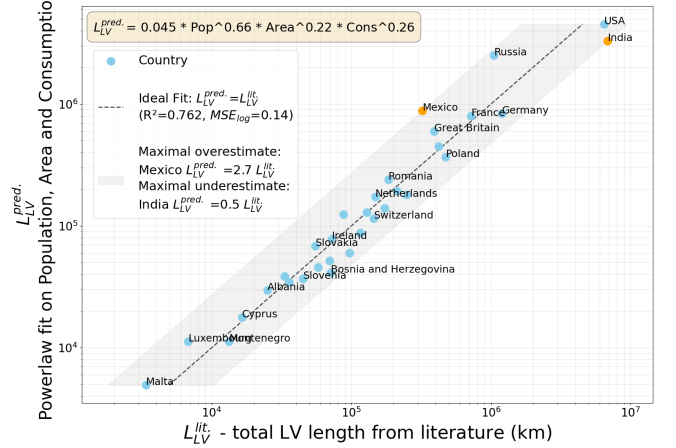


Figure 9: Estimation of total L_{LV} value using powerlaw relationship on country’s total population and area.

D. Material investment scaling with network length

Having a heuristic for the total cable length enables an inventory of the material invested. We use copper as an example in the following, but the method is the same for other materials. Using the Surfer database from ADEME [5], we can get consensual values of material intensities for power grid lines. The copper intensity of MV line is $\xi_a \simeq 1.49 \text{ t/km}$ for aerial lines and $\xi_u \simeq 0.96 \text{ t/km}$ for underground lines. After we build the network, multiplying the total MV length by ξ_u gives us a lower bound (resp. multiplying by ξ_a for an upper bound) of the total amount of copper invested in lines. This is shown in figure 11.

Another way, even more straightforward, is to use macro-level indicators for material estimates. In this regard, the equation 5 could be converted in a copper mass

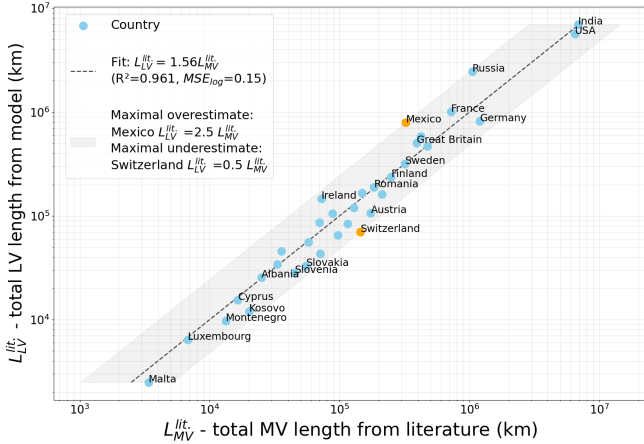


Figure 10: Estimation of total L_{LV} value using linear regression on L_{MV} value.

estimator:

$$m_{C_u}^{MV} = 0.17 \text{Pop}^{0.59} \text{Area}^{0.36} \times (\xi_u \tau + \xi_a (1 - \tau)) \quad (7)$$

where τ is the fraction of underground cable. The value of τ is hard to model and varies dramatically across countries and regions, driven by regulatory frameworks, aesthetic considerations, and economic factors. The same method could be applied to the LV layer. However, the vast majority of the LV copper is for the underground case, so the uncertainties on τ become critical.

IV. DISCUSSION & CONCLUSION

We have developed a simple modeling approach that simulates the spatial distribution of medium-voltage substations from high-resolution population density fields. From this point distribution, we derive an approximation of the associated MV network topology, yielding a refined estimate of the total cable length. The WorldPop database provides such population density data for each country and for each year between 2000 and 2020, and our method has been validated across more than 30 countries spanning various territorial specificities.

By inputting high-resolution population data in our network-generation algorithm, we can localize copper infrastructure at the square-kilometer scale. This fine-grained spatial information supports targeted material flow analysis and territorial planning, enabling the identification of where metallic resources are concentrated within the distribution grid. These results are particularly relevant to global electrification scenarios and infrastructure planning. For instance, the work of Vidal *et al.* on future energy infrastructure requirements highlights the need for robust methods to estimate distribution network expansion [27]. Such methods can be applied in emerging economies where detailed grid records are scarce, enabling forecasts of infrastructure and material needs accompanying electrification.

This local-scale framework also serves as the foundation for analyzing global scaling properties of electricity distribution networks. We conducted a multivariate analysis to estimate properties of the MV/LV grid from macro-level indicators. A remarkable finding is that electricity consumption can be omitted from the scaling relationships for medium-voltage network length without significantly degrading predictive accuracy. This suggests that, at the national scale, the spatial distribution of population and territorial extent captures the primary drivers of network extent, while the consumption effect is negligible. This observation may reflect an emergent property of distribution networks: once population distribution and territorial extent are specified, the MV network topology is largely determined by the spatial optimization required to connect distributed loads. However, we show that this is not the case for the LV layer, where consumption contribution remains important. This effect is not surprising: the infrastructure used to supply households is always short-distance at this scale, and power capacity satisfaction is the only constraint.

Taken together, these results demonstrate that realistic distribution grid structures can be generated solely from population density, and that aggregate network characteristics follow predictable scaling relationships with population and area. These findings provide new multi-scale tools for characterizing electrical infrastructure and reveal that population spatial distribution is a key determinant of distribution grid extent. From this understanding, these tools can be generalized in many ways.

First, the network-generative process can be extended to the LV layer, branching the MV/LV substations down to end consumers. In this direction, high-resolution topographic databases such as the French BD TOPO [28], which provides a precise description of buildings and infrastructure across the national territory, could help to calibrate the spatial distribution of end-user connection points. In the end, this would yield a complete, end-to-end representation of the distribution network and refine material-requirement estimates, particularly for the copper-intensive last-kilometer segments.

Second, regarding temporal extension, the model could be adapted to population density time series to estimate the temporal evolution of the French grid. However, this approach relies on the assumption that the identified relationship was also valid in the past, an assumption that cannot be verified in the absence of sufficiently detailed historical data. It could nonetheless yield useful results for long-term studies—for instance, to describe the historical deployment of the French grid and to anticipate forthcoming replacement waves [29]—albeit subject to a strong underlying assumption. From a prospective perspective, the model appears considerably more suitable, as the current grid configuration likely reflects a degree of maturity and optimality that may persist into the future, thereby maintaining the descriptive power of the relationship. It is nevertheless important to emphasize the potential for major decentralization of electricity genera-

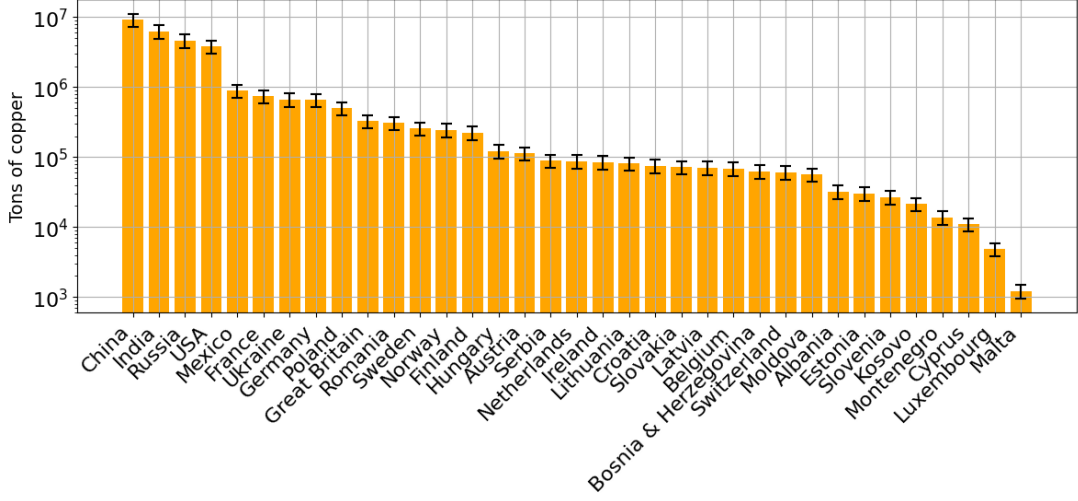


Figure 11: Approximation of the total amount of the copper invested in MV grid for various countries using corrected length values from the network algorithm. The upper bound is reached if there are only aerial lines, and the lower bound is reached if there are only underground lines.

tion driven by the expansion of renewable energy sources, which could affect the distribution network and alter the observed empirical relationship.

Third, we can note that population density fields could serve as a common generation parameter for other infrastructure networks (water distribution, gas pipelines, or telecommunications, for instance) whose deployment logic is likewise driven by the spatial distribution of demand. Then, adapting the substation-sampling and network-construction steps to the specific technological constraints of each system would open the way to multi-layer infrastructure modeling and to extended analyses of material needs.

Acknowledgements—We would like to acknowledge interesting discussions with Charley Presigny, Sourin Chatterjee and Seddik Yassine Abdelouadoud.

Author contributions—JH supervised this work. EE and JLB performed the investigation, formal analysis, software development, initial draft writing, final writing, review, and editing equally. All authors contributed to the study’s conceptualization and validation.

Conflict of interest—The authors have no conflict of interest to declare.

Data availability—The data used are open-access data [11, 16] or referenced in appendix C.

Code availability—The code developed for this paper is available at <https://doi.org/10.5281/zenodo.18634548>.

Funding— Research funded via PEPR Recyclage.

Appendix A VORONOI SLICING

We can optimize the cell layout using Voronoi cells as illustrated in Figure 12. Each Voronoi cell is centered on a substation s , and its boundaries delimit the fraction of the total area that is closer to the substation s than to the other substations. Thus, each cell contains exactly one node, but varies in size. Given this cell layout, Figure 13 illustrates that the strong rupture of the slope disappears. The two regimes appearing in Equation (1) seem to be artifacts of the artificial grid-cell lattice. The Voronoi grid seems to better capture the effective layout of substations. However, the fine-grained datasets that we use are based on a regular lattice spatial grid.

Appendix B CORRECTION TO THE MINIMUM SPANNING TREE

After we sample a spatial repartition of nodes, we estimate the kilometers of distribution lines needed to connect them. Since we are dealing with estimates only, we can use the *minimum spanning tree* (MST) algorithm to connect the lines with the minimum total length. That said, the Kruskal process that we take is radical, and some corrections are needed to improve precision.

- The MST lines are straight lines (distance “as the crow flies”). In reality, for practical reasons (like efficiency of building and maintenance), many distribution lines follow the road network [7] whose

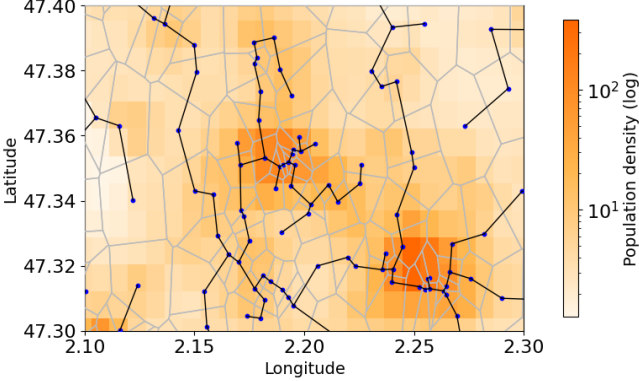


Figure 12: Real population density data in France (orange) with simulated nodes (blue), minimum spanning tree edges (black), and computed Voronoi diagram (grey).

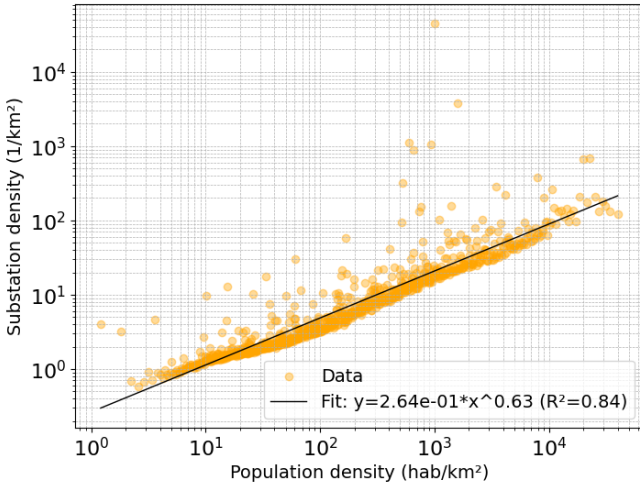


Figure 13: Same as Figure 1 but with a Voronoï cell layout.

topology can be approximated by a square lattice [30]. Assuming the distribution network maintains this square shape, we need to add a correction factor to account for the average rescaling between Manhattan and Euclidean distances. As depicted in Figure 14, the correspondence between the Manhattan distance L_M and the Euclidean distance L_E given an angle α relative to the embedded square is:

$$L_M(\alpha) = (\cos \alpha + \sin \alpha)L_E. \quad (8)$$

Averaging over α , this yields:

$$\langle L_M \rangle_\alpha = \frac{2}{\pi} \int_0^{\frac{\pi}{2}} L_M(\alpha) d\alpha = \frac{4}{\pi} L_E, \quad (9)$$

leading to the first correction factor $\gamma_1 = \frac{4}{\pi}$.

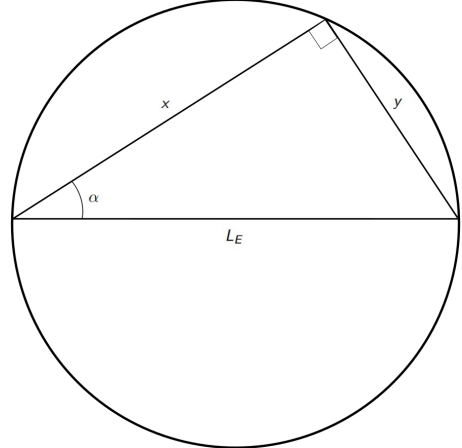


Figure 14: Drawing of the difference between Manhattan distance $L_M = x + y$ and Euclidean distance L_E given an angle α .

- The uncorrected MST length value is for the routes (the pillar paths), which can contain more than one cable. To estimate material investments, we need to determine the cable length required for the simulated network. The ENEDIS open database provides access to line-shaped cable data as a set of areas corresponding to cable segments. For each cable segment of length ℓ_i , the dataset contains a formal surface a_i corresponding to the full surface within 5 meters of the line. Even though it is not rich enough to reconstruct a topology, this geographical data can be used to measure distances precisely. The total cable distance is the sum of all the line-shaped cable data:

$$L_{\text{cab}} = \sum_{i=1}^{N_d} \ell_i, \quad (10)$$

with N_d the number of line-shaped entries. For the ENEDIS dataset, we get for the underground and aerial MV lines:

$$L_{\text{cab}}^{\text{aer}} = 330\,996 \text{ km}, \quad L_{\text{cab}}^{\text{und}} = 376\,527 \text{ km}. \quad (11)$$

This includes the overlaps. Using $|a|$ as the notation for the area of the surface a , we can estimate globally the total surface A spanned by the a_i with overlap included and the total surface A' spanned by the a_i with overlaps excluded (overlap will artificially increase the area spanned by cables):

$$A = \sum_{i=1}^{N_d} |a_i|, \quad A' = \left| \bigcup_{i=1}^{N_d} a_i \right|. \quad (12)$$

To factor out the overlap contribution in the total length estimates, we build a rescaled L_{route} such that

$$L_{\text{route}} = \frac{A'}{A} L_{\text{cab}}. \quad (13)$$

We now estimate the real-world length of the distribution with overlap excluded:

$$L_{\text{route}}^{\text{aer}} = 321\,629 \text{ km}, \quad L_{\text{route}}^{\text{und}} = 299\,518 \text{ km.} \quad (14)$$

We remark that most of the overlaps concern the underground edges: tunnels are dug to gather many cables. Having this done, we estimate the route-to-cable correction factor (calibrated on the French MV layer) as $\gamma_2 \simeq 1.139$.

- The MST is a lower bound; in reality, there are some bridge edges causing loops in the MV layer. Comparing the data with the model, this could explain the remaining factor $\gamma_3 \simeq 1.060$. To implement this partially looped structure, we can generalize the Kruskal algorithm as follows, taking as input a set of spatial nodes with their coordinates, and a parameter b . First, add all possible edges to

form a clique network G from the input node locations. Secondly, for each edge (i, j) in decreasing length order, we check if removing (i, j) will make the shortest path from i to j higher than b . If so, we keep (i, j) , otherwise, we delete it from the network.

All these informations could be included in a factor $\gamma = \gamma_1 \gamma_2 \gamma_3 \simeq 1.537$ such that the total length of MV lines yields:

$$L_{\text{MV}} = \gamma L_{\text{MST}}. \quad (15)$$

Appendix C DATA SOURCES

The sources of the literature values used in subsections III B and III C are detailed in table II.

[1] G. Kalt, P. Thunshirn, D. Wiedenhofer, F. Krausmann, W. Haas, and H. Haberl, Material stocks in global electricity infrastructures – An empirical analysis of the power sector’s stock-flow-service nexus, *Resources, Conservation and Recycling* **173**, 105723 (2021).

[2] IEA, Electricity grids and secure energy transitions (2023).

[3] V. Crastan, *Les réseaux d’énergie électrique - Volume 1* (Librairie Eyrolles, 2006).

[4] E. Emery, S. Aumaître, and H. Bercegol, Power Grid Network Growth Model Based on Rural-Urban Differentiation, *PRX Energy* **4**, 033014 (2025).

[5] D. Monfort, F. Laurent, H. L. Boulzec, G. Lefebvre, B. Rodriguez, S. Muller, C. François, B. Andrieu, O. Vidal, and J. Villeneuve, Projet surfer, inventaires des besoins en matière, énergie, eau et sols des technologies de la transition énergétique., ADEME (2020).

[6] A. Zvoleff, A. S. Kocaman, W. T. Huh, and V. Modi, The impact of geography on energy infrastructure costs, *Energy Policy Carbon in Motion: Fuel Economy, Vehicle Use, and Other Factors affecting CO2 Emissions From Transport*, **37**, 4066 (2009).

[7] C. Arderne, C. Zorn, C. Nicolas, and E. E. Koks, Predictive mapping of the global power system using open data, *Scientific Data* **7**, 19 (2020).

[8] H. Persoz, *La Planification des réseaux électriques*, Collection de la Direction des études et recherches d’Électricité de France No. 50 (Eyrolles, Paris, 1984).

[9] G. A. Pagani and M. Aiello, A complex network approach for identifying vulnerabilities of the medium and low voltage grid, *International Journal of Critical Infrastructures* **11**, 36 (2015).

[10] S. Dunn, S. Wilkinson, and A. Ford, Spatial structure and evolution of infrastructure networks, *Sustainable Cities and Society* **27**, 23 (2016).

[11] WorldPop, Global high resolution population denominators project (2018).

[12] A. E. Gaughan, F. R. Stevens, Z. Huang, J. J. Nieves, A. Sorichetta, S. Lai, X. Ye, C. Linard, G. M. Hornby, S. I. Hay, H. Yu, and A. J. Tatem, Spatiotemporal patterns of population in mainland China, 1990 to 2010, *Scientific Data* **3**, 160005 (2016).

[13] A. Sorichetta, G. M. Hornby, F. R. Stevens, A. E. Gaughan, C. Linard, and A. J. Tatem, High-resolution gridded population datasets for Latin America and the Caribbean in 2010, 2015, and 2020, *Scientific Data* **2**, 150045 (2015).

[14] F. R. Stevens, A. E. Gaughan, C. Linard, and A. J. Tatem, Disaggregating Census Data for Population Mapping Using Random Forests with Remotely-Sensed and Ancillary Data, *PLOS ONE* **10**, e0107042 (2015).

[15] ENEDIS, Plaquette institutionnelle (2023).

[16] ENEDIS, Cartographie des réseaux exploités par Enedis (2024).

[17] F. Gonzalez Venegas, *Electric Vehicle Integration into Distribution Systems*, Ph.D. thesis, Université Paris-Saclay (2021).

[18] V. Crastan, *Les réseaux d’énergie électrique - Volume 2* (Librairie Eyrolles, 2007).

[19] S. Abeysinghe, J. Wu, M. Sooriyabandara, M. Abeysekera, T. Xu, and C. Wang, Topological properties of medium voltage electricity distribution networks, *Applied Energy* **210**, 1101 (2018).

[20] World Bank, Access to electricity (% of population) – SDG 7.1.1 electrification dataset, <https://trackingsdg7.esmap.org/downloads> (2023).

[21] E. Blauvelt, *Transformer Report Edition 9*, Tech. Rep. (StatPlan Energy Research, 2021).

[22] G. Kalt, P. Thunshirn, and H. Haberl, A global inventory of electricity infrastructures from 1980 to 2017: Country-level data on power plants, grids and transformers, *Data in Brief* **38**, 107351 (2021).

[23] L. M. A. Bettencourt, J. Lobo, D. Helbing, C. Kühnert, and G. B. West, Growth, innovation, scaling, and the pace of life in cities, *Proceedings of the National Academy of Sciences* **104**, 7301 (2007).

[24] C. Kühnert, D. Helbing, and G. B. West, Scaling laws in

urban supply networks, *Physica A: Statistical Mechanics and its Applications Information and Material Flows in Complex Networks*, **363**, 96 (2006).

[25] L. M. A. Bettencourt, The Origins of Scaling in Cities, *Science* **340**, 1438 (2013).

[26] A. Cattaneo, A. Adukia, D. L. Brown, L. Christiaensen, D. K. Evans, A. Haakenstad, T. McMenomy, M. Partridge, S. Vaz, and D. J. Weiss, Economic and social development along the urban–rural continuum: New opportunities to inform policy, *World Development* **157**, 105941 (2022).

[27] O. Vidal, H. Le Boulzec, B. Andrieu, and F. Verzier, Modelling the Demand and Access of Mineral Resources in a Changing World, *Sustainability* **14**, 11 (2021).

[28] IGN, *Bd TOPO* (2025).

[29] J. L. Bihani, T. Lapi, and J. Halloy, Modeling technological deployment and renewal: monotonic vs. oscillating industrial dynamics, *PLOS Sustainability and Transformation* **4**, e0000205 (2025).

[30] M. Barthélémy, *Spatial Networks: A Complete Introduction* (Springer Nature, Cham, Switzerland, 2022).

Category / Country	Type of Data	Source / URL
General	L_{MV}	https://www.ceer.eu/wp-content/uploads/2024/04/7th-Benchmarking-Report-2022.pdf
General	Number of households, Electric energy consumption	World Bank
Great Britain	L_{MV}, N_{stat}	https://assets.publishing.service.gov.uk/government/uploads/system/uploads/attachment_data/file/479267/climate-adrep-ena-2015.pdf https://www.ofgem.gov.uk/publications/2008-2009-electricity-distribution-quality-service-data-tables
Slovakia	L_{MV}, N_{stat}	https://www.tdworld.com/overhead-distribution/article/20962833/distributed-generation-drives-system-planning https://www.ssd.sk/buxus/docs/dokumenty/o_nas/vyrocne_spravy/Vyrocna%20sprava%20a%20uctovna%20zavierka%202017%20SSD.pdf https://www.atpjournal.sk/buxus/docs/dokumenty/kniznica_dokumentov/2014/Horak_ZSDS.pdf
Germany	N_{stat}	https://www.geode-eu.org/wp-content/uploads/2024/06/Grids-for-Speed_Report.pdf
Estonia	N_{stat}	https://www.energia.ee/-/doc/8457332/ettevottest/aastaaruanne2018/EE_Annual_report_2018.pdf
USA	L_{MV}, L_{LV}, N_{stat}	https://www.energy.gov/sites/prod/files/2021/03/f83/Advanced%20Transmission%20Technologies%20Report%20-%20final%20as%20of%2012.3%20-%20FOR%20PUBLIC_0.pdf https://www.statplanenergy.com/wp-content/uploads/2021/08/Transformer-Report-Chapter-Summaries-TOC-Sample-Pages-Ed-9-2021.pdf https://www.energy.gov/sites/prod/files/2017/01/f34/Electricity%20Distribution%20System%20Baseline%20Report.pdf
India	L_{MV}, L_{LV}, N_{stat}	https://www.ceicdata.com/en/india/electricity-number-of-transformers https://now.solar/2021/04/07/growth-of-electricity-sector-in-india-from-1947-2020/
China	L_{MV}, L_{LV}, N_{stat}	https://ptr.inc/demystifying-chinas-power-grid/ https://chinaenergyportal.org/en/2018-detailed-electricity-statistics-update-of-dec-2019/
Russia	L_{MV}, L_{LV}, N_{stat}	[22]; https://www.cigre.org/userfiles/files/Community/National%20Power%20System/Pr%C3%A9sentation%20PowerPoint%20-%202020_National_power_system_RUSSIA.pdf https://www.cigre.org/userfiles/files/Community/NC/Russia.The_Electric_Power_System.pdf
Mexico	L_{MV}, L_{LV}, N_{stat}	https://www.cenace.gob.mx/Docs/Planeacion/ProgramaRNT/Programa%20de%20Ampliaci%C3%B3n%20y%20Modernizaci%C3%B3n%20de%20la%20RNT%20y%20RGD%202019%20-%202033.pdf https://www.proyectosmexico.gob.mx/wp-content/uploads/2018/09/VIIN-FINAL.pdf https://base.energia.gob.mx/prodesen/PRODESEN2018/PRODESEN18.pdf

Table II: Summary of data sources used for grid length and related indicators